Applied Computing and Informatics (2015) **11**, 13–28

Saudi Computer Society, King Saud University

**Applied Computing and Informatics**

(http://computer.org.sa)
www.ksu.edu.sa
www.sciencedirect.com

ORIGINAL ARTICLE

# Inverse spiking filter based acquisition enhancement in software based global positioning system receiver

**G. Arul Elango *, G.F. Sudha, Bastin Francis**

*Department of Electronics and Communication Engineering, Pondicherry Engineering College, Puducherry, India*

Received 11 July 2013; revised 23 January 2014; accepted 22 February 2014
Available online 28 February 2014

**KEYWORDS**

GPS;
Inverse spiking filter;
Differential coherent detection;
Weak signal acquisition

**Abstract** The lower visibility of the satellite in the acquisition stage of a GPS receiver under worst noisy situation leads to reacquisition of the data and thereby takes a longer time to obtain the first position fix. If the impulse noise affects the GPS signal, the conventional ways of acquiring the satellites do not guarantee to meet the minimum requirement of four satellites to find the user position. The performance of GPS receiver acquisition can be improved in the low SNR level using inverse spiking filtering technique. In the proposed method, the estimate of the desired GPS L1 signal corrupted by impulse noise ($g_n$) is obtained by the prediction error filter ($h_{opt}$), which is the optimum inverse filter that reshapes the noisy signal ($y_n$) into a desired GPS signal ($x_n$). In the proposed method, to detect the visible satellites under weak signal conditions the traditional differential coherent approach is combined with the inverse spiking filter method to increase the number of visible satellites and to avoid the reacquisition process. Montecarlo simulation is carried out to assess the performance of the proposed method for $C/N_0$ of 20 dB-Hz and results indicate that the modified differential coherent method

* Corresponding author. Tel.: +91 8220728835.
E-mail addresses: arulelango2012@gmail.com (G. Arul Elango), gfsudha@pec.edu (G.F. Sudha), bastinfrancis@gmail.com (B. Francis).

Peer review under responsibility of King Saud University.

Production and hosting by Elsevier


http://dx.doi.org/10.1016/j.aci.2014.02.002

effectively excises the noise with 90% probability of detection. Subsequently tracking operation is also tested to confirm the acquisition performance by demodulating the navigation data successfully.



## 1. Introduction

At present GNSS (Global Navigation Satellite System) consists of two fully operational global systems, the United States' global positioning system (GPS) and Russia's GLObal NAvigation Satellite System (GLONASS), as well as the developing global and regional systems, namely Europe's European Satellite Navigation System (GALILEO), China's COMPASS/Bei-Dou, India's Regional Navigation Satellite System (IRNSS) and Japan's Quasi-Zenith Satellite System (QZSS). GPS is used in a large number of safety critical applications and has become essential for precise timing reference and synchronization purpose in telecommunications networks (Zhu et al., 2010). GPS signal power levels are extremely low, due to the long satellite-receiver distance. The commercial GPS receiver is easily affected by vulnerable effects of interference and noise. The GPS receiver mounted on or inside manned or autonomous vehicles is easily affected by impulse noise caused by motor emissions. This leads to a drop in the carrier power to noise density ratio. Hence, it is important to have an effective method to detect and filter the noise. Spectral signal processing consists of time and frequency excision, pulse blanking and pulse spiking techniques which are used to prevent loss of lock caused by the effect of noise (Borio et al., 2008).

The nominal power level of the received signal is only −158.5 dBW. The highest power density of the spread spectrum signal is −220 dBW/Hz where the nominal background noise level is approximately −205 dBW/Hz, i.e. the signal strength lies 15 dB under the background noise level (Braasch and Van Dierendonck, 1999). A GPS signal below −158.5 dBW power level is categorized as a weak signal, so there is a strong possibility of the cross-correlation peaks exceeding the autocorrelation peaks. This will ruin acquisition and reduce satellite availability. The pre-detection integration time plays a vital role in signal detection and in determining the feasible gain. This should be optimally selected to achieve the desired acquisition sensitivity with the available processing power and to avoid false locks. Hence the detection threshold should be optimally chosen to avoid false locks which can be achieved by selecting a proper value of the false detection probability (Hu and Fang, 2010). To find the weak signal, the approach is to increase the data length. Three approaches based on the integration time namely coherent, non-coherent and differential coherent techniques are used during the weak signal

acquisition in order to improve the SNR. Dividing the set of input data into smaller blocks then stripping the C/A code from the data and performing FFT based parallel code phase search technique (performing an algebraic sum of the signal) are known as coherent detection (Bao-Yen and Tusi, 2005). In the non coherent integration method, summing the data blocks of squared correlation values of the acquisition process (performing an absolute sum of the signal) yields good correlation. This increases the signal strength by a factor of 2 and noise by $\sqrt{2}$ thereby increasing the SNR by $\sqrt{2}$ or 1.5 dB (Deshpande et al., 2004). This improvement is less compared to the coherent integration method but requires fewer operations. Also non-coherent integration is not affected by the navigation data bit transition since the correlation results of the coherent integration time are squared before summation. When the correlator output is multiplied with the complex conjugate of the successive correlator output this method is termed as differential coherent detection and thus by doing this a high degree of correlation is being maintained. Hence, the SNR loss in differentially combining detection is decreased in comparison to non-coherent combining detection. Fallahi et al. (2012) calculated probability of detection and the ROC (Receiver Operating Characteristic) using coherent, non-coherent and differential detection at various power levels of GPS signal.

The typical $C/N_0$ value of a commercial GPS receiver is in between 37 and 45 dB-Hz. In the noisy environment of analyzing the GPS signal, the traditional methods of coherent, non coherent and differential coherent ways of increasing the integration time result in poor correlation. If the impulse noise distorts the GPS signal, the parallel code phase search acquisition performed for single msec data works only for $C/N_0$ up to 35 dB-Hz of the GPS receiver. Hence, it is quite obvious to use the coherent integration method for the lower $C/N_0$ in the range of 35 dB-Hz and the non-coherent integration method with $C/N_0$ up to 30 dB-Hz (Deshpande et al., 2004). A longer coherent integration time means a smaller Doppler bin size which increases the number of the Doppler bins to be searched. The coherent integration time is limited by two factors, navigation data bit transition and the Doppler effect on the C/A-code. A navigation data bit transition will spread the spectrum causing the output to be no longer a CW signal. This spectrum spreading will reduce the acquisition gain and distort the acquisition peak. An increase of 100 ms non coherent integration correlation can acquire the signal having $C/N_0$ up to 25 dB-Hz. But all the above mentioned techniques cannot be applied for impulse noise affected GPS signal which has $C/N_0$ less than 20 dB-Hz. In this paper, it is proposed to excise the impulse noise embedded in the GPS signal with $C/N_0$ below 20 dB-Hz through the inverse spiking filtering technique. The structure of the paper is organized as follows. This section discusses the existing methods available for weak signal acquisition. Section 2 describes the mathematical formulation and theory of inverse spiking filter, Section 3 illustrates the acquisition and tracking results of conventional and the proposed modified differential methods of processing the noisy GPS signal as well as Montecarlo

simulation is also performed to confirm the effectiveness of the acquisition process. Section 4 gives the conclusions.

## 2. Inverse spiking filter based noise excision in GPS receiver

In this section, the spiking inverse filter based noise excision is proposed for excising the impulse noise. The received noisy GPS L1 signal which has a $C/N_0$ below 20 dB-Hz is subjected to the spiking filter and the output of the spiking filter is given to the A/D converter with a sampling frequency of 11.999 MHz .If 1 ms of data is analyzed, the number of samples can be found as 1/1000 of the sampling frequency ($11.999 \times 10^6/1000 = 11{,}999$ samples) with a single bit resolution (Bao-Yen and Tusi, 2005). The digitized data obtained after A/D is given as an input to the acquisition process with peak search algorithm.(Mao et al., 2008).

The impulse noise ($g_n$) and the GPS signal ($x_n$) are related by the convolution relationship

$$y_n = x_n * g_n = \sum_m g_m x_{n-m} \tag{1}$$

The basic objective here is to recover $x_n$ from impulse noise affected signal $y_n$.

The spiking de-convolution (Mathew and Narayana Dutt, 1993) is proposed to compress the effect of impulse noise embedded in the GPS signal and to improve the SNR value. The problem may be formulated as follows: To design a spiking inverse filter $h_n$ corresponding to the impulse noise function $g_n$, that is, $h_n * g_n = \delta_n$. In the least-squares sense filtering $y_n$ through $h_n$ will recover the desired signal $x_n$. If the given record of available noisy GPS data is $y_n = \{y_0, y_1, y_2 \ldots., y_N\}$, then the inverse spiking filter coefficients $h_n = \{h_0, h_1, h_2 \ldots. h_M\}$, will reshape $y_n$, into the desired GPS signal $x = \{x_0, x_1, x_2 \ldots., x_N\}$. The estimate of input signal is given by the convolution relationship (Orfanidis, 1988).

$$\hat{x}_n = \sum_m y_{n-m} h_m \tag{2}$$

and the estimation error becomes,

$$e = x - \hat{x}_n \tag{3}$$

As the optimality criterion, least square criteria aregiven by $J_{\min} = \|e^2\| = e^T e$

In compact matrix form Eq. (2) can be written as

$$\hat{x} = Yh \tag{4}$$

where Y is the (N + M + 1) × (M + 1) convolution matrix data matrix from the noisy signal $y_n$ and $x$ is the (N + M + 1)×1 vector of estimate of input samples.

$$Y = \begin{bmatrix} y_0 & 0 & 0 & \cdots & 0 \\ y_1 & y_0 & 0 & \cdots & 0 \\ y_2 & y_1 & y_0 & \cdots & 0 \\ \vdots & \vdots & \vdots & \vdots & \vdots \\ y_N & y_{N-1} & y_{N-2} & \cdots & y_{N-M} \\ 0 & y_N & y_{N-1} & \cdots & y_{N-M+1} \\ 0 & 0 & y_{N-1} & \cdots & y_{N-M+2} \\ \vdots & \vdots & \vdots & \cdots & \vdots \\ 0 & 0 & 0 & 0 & y_N \end{bmatrix}$$

Using the orthogonality condition

$$Y^T e = Y^T(x - Yh) = 0$$

(Or) $Y^T Yh = Y^T x$, solving for h this equation becomes

$$h = (Y^T Y)^{-1} Y^T x = R^{-1} r \tag{5}$$

The actual filter output $\hat{x}$ is expressed as

$$\hat{x} = Yh = Y(Y^T Y)^{-1} Y^T x = Px \quad \text{where } P = YR^{-1} Y^T$$

The error vector can be written as

$$e = (1 - \mathrm{P})x \tag{6}$$

The error square becomes

$$J = \|e^2\| = e^T e = x^T(I - P)x \tag{7}$$

The "performance" matrix $P$ is a projection matrix with size (N + M + 1) × (N + M + 1) and has trace equal to M + 1, while its eigenvalues are either 0 or 1.For the sum of all the eigenvalues to be equal to M + 1, there should be M + 1 eigenvalues that are equal to 1, and N eigenvalues equal to 0. Therefore, the matrix $P$ has rank M + 1 (Mathew and Narayana Dutt, 1993), and if the desired vector $x$ is selected to be any of the M + 1 eigenvectors belonging to eigenvalue 1; the resultant estimation error will be zero. The desired vector $x$ is chosen as spikes or impulse i.e. $x = \delta_n$. Here $h$ is the best least squares approximation that reshapes $y_n$ into a unit impulse. Considering the vector $x$ to be a unit impulse occurring at the i-th instant, $x = \delta(n - \mathrm{i})$.

The actual filter output from the spiking filter is given by

$$\hat{x} = Px = P\delta(n - i) \tag{8}$$

Thus the i-th column of $P$ matrix is the output of the i-th spiking filter which reshapes $y_n$ into a spike with $i$ delays. The corresponding i-th filter is

$$h_{\text{opt}} = R^{-1} Y^T \delta(n - i) \tag{9}$$

Hence the columns of the matrix $R^{-1}Y^T$ are all the optimal spiking filters. The estimation error of the i-th filter is

$$J = [\delta(n-i)]^T(I-P)\delta(n-i) = 1 - P_{ii} \tag{10}$$

where $P_{ii}$ represents the i-th diagonal entry of the projection matrix. Once the matrix of inverse filters is computed, the optimum among them is selected as the one which has the smallest error. Since the delay $i$ may be positioned anywhere from $i = 0$ to $i = \mathrm{N} + \mathrm{M}$, there are $\mathrm{N} + \mathrm{M} + 1$ such spiking filters, each with error $J$. The filter which has the optimal delay $i$ corresponds to the smallest of the error $J$ or, equivalently, to the maximum of the diagonal elements $P_{ii}$. The particular column $i$ of $P$ for which $P_{ii}$ is maximum will give the extracted data; The corresponding system model is shown in Fig. 1.

The steps involved in least-squares spiking filter design for a given signal $y_n$, $n = 0, 1\ldots, N-1$ are summarized as follows:

1. Construct an autocorrelation matrix ($Y^TY$).
2. Calculate all inverse filters through pseudo inverse of an autocorrelation matrix.
3. Find i-th diagonal entry of a projection matrix which has maximum value.
4. Obtain i-th filter i.e. $h_{\mathrm{opt.}}$
5. Extract the data $\hat{x}$ by convolving $h_{\mathrm{opt}}$ with noisy signal $y_n$.

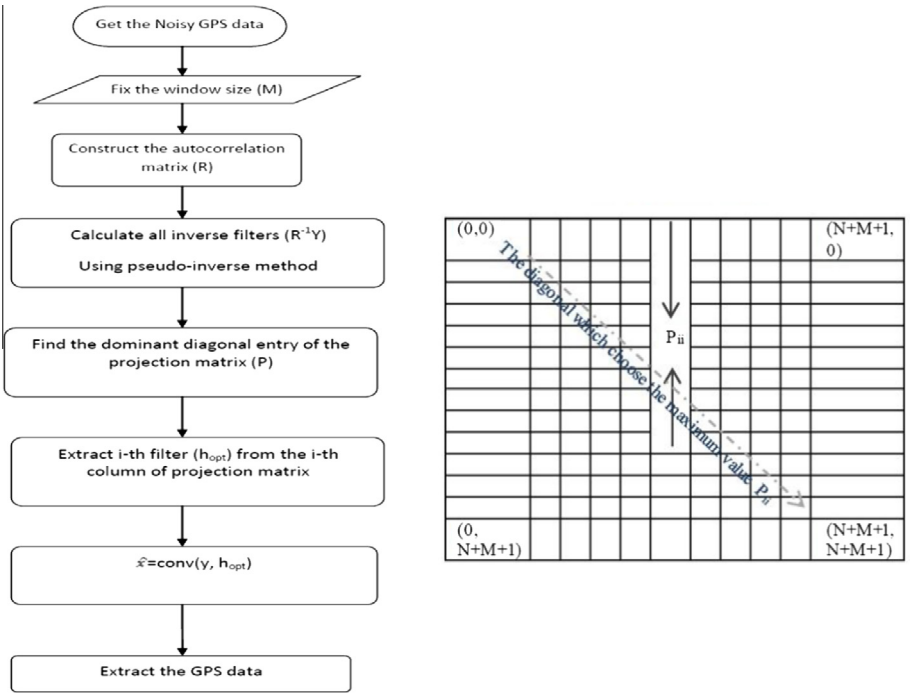


**Figure 1** System model for the inverse spiking filter design and the performance matrix.

The performance of the spiking filter is determined by the diagonal values of the performance matrix $P$. Based on the minimum mean square error value, the particular diagonal entry has a maximum value that determines the rank of the matrix (Mathew and Narayana Dutt, 1993).

## 3. Experimental results

### *3.1. Software based GPS receiver acquisition performance assessment in the presence of impulse noise*

The GPS signal affected by the impulse noise with $C/N_0$ of 20 dB-Hz is given to the proposed filter model. The filtered data are passed through an acquisition block of peak search algorithm. As per the simulation parameters for the GPS L1 signal mentioned in Table 1, the acquisition performances are tested for three different scenarios and the outputs are tabulated in Table 2. For all the 3 cases the peak algorithm proposed by Mao et al. (2008) has been used. The threshold condition is set based on the maximum peak and the secondary peak values of the decision statistic (S) in the acquisition process. The Threshold Condition used for simulation is given as the Correlation max Peak – Mean Peak > 0.96 and the Max Peak – Secondary Peak > 0. 5. Based on this condition, the simulation is carried out for single msec data, and it is observed that the signal is absent due to poor SNR and the typical parallel code phase search algorithm fails to detect the distinct peak. Hence longer msec data of coherent integration are used for improving the SNR of the signal, but there is no significant improvement in stripping the noise. On the other hand, even if non-coherent integration is performed, the acquisition success percentage does not improve due to the large false alarm peaks. The minimum requirement of 4 visible satellites was not attained in both coherent and non coherent integration methods. Finally the spiking filter combined with the differential coherent detection method is tested and it is able to suppress the impulse noise and able to locate more number of visible satellites. Table 2 shows the Satellite Vehicle Number (SVN) that is visible using the proposed method.

**Table 1** Acquisition simulation parameters for GPS signal subjected to the impulse noise.

| Parameters | Values |
|---|---|
| Order of filter/window size ($M$) | 50 |
| Input sample data length($n$) | 11,999 |
| Centre frequency ($f_{c0}$) | 3.563 MHz |
| Sampling frequency ($f_s$) | 11.999 MHz |
| Doppler frequency search ($f_d$) | $\pm$10 kHz |
| Search steps | 41 |
| Integration time (coherent, non-coherent, differential coherent) | 10 ms, 36 ms, 12 ms |

The GPS signal and its corresponding spectrum are shown in Fig. 2a and b respectively. Impulse noise power level of 12 dB is mixed with GPS L1 signal and it is excised through spiking filter are shown in Fig. 2c and d. The spectrum of the retrieved signal resembles the original signal spectrum and the noisy signal power spectral density as shown in Fig. 2e and f.

The performance metric of the spiking filter is determined by the maximum diagonal entry in a performance matrix or the error function $(1 - P_{ii})$ with respect to the order of the filter which is shown in Fig. 3a and the impulse response of the spiking filter of order 50 is illustrated in Fig. 3b.

The acquisition result of SVN-16 obtained by the conventional methods for single msec, coherent, non-coherent and differential coherent detection for the noisy data is shown in Fig. 4.This depicts that the start of C/A code is not perfectly aligned with the incoming signal C/A code due to the many cross correlation peaks that exceed the autocorrelation peaks. So the above mentioned traditional methods fail to detect the decision statistic or threshold condition of the visible satellite. Processing of single msec data results in worst correlation. Similarly analyzing of coherent and non-coherent detection also provides many cross correlation peaks. By comparing the outputs in Fig. 4, the conventional differential coherent approach gives a better performance of detecting SVN-16. Only 2 SVNs surpass the threshold condition but minimum 4 SVNs are required to find the user position.

Next the same noisy data are tested with the spiking filter combined with differential coherent detection (modified differential coherent). Increased visibility of the satellites [SVN 3, 9, 10, 13, 16, 23 and 30] in terms of distinct peak (perfect alignment with C/A code) is shown in Fig. 5. This approach performs better compared to other traditional methods and ensures that the corrected code phase and Doppler frequency enhance the acquisition performance. The results of Table 3 show the visible satellites, their respective Doppler frequency and code phase.

### *3.2. Determination of acquisition success percentage using Montecarlo simulation*

To examine the acquisition performance under noisy condition, all conventional methods are tested using Montecarlo simulation. In this simulation, the locally

**Table 2** Simulation results of comparison for different techniques used in longer msec data.

| Conventional methods | | | | Proposed method |
|---|---|---|---|---|
| Single msec data | Coherent (10 ms data) | Non coherent (36 ms data) | Differential coherent (12 ms data) | Modified differential coherent (12 ms data) |
| No visible Satellites (needs re-acquisition of GPS data) | | | 2 visible Satellites [SVN 13, 16] (needs re-acquisition of GPS data) | 7 visible Satellites [SVN 3, 9, 10, 13, 16, 23 and 30] |

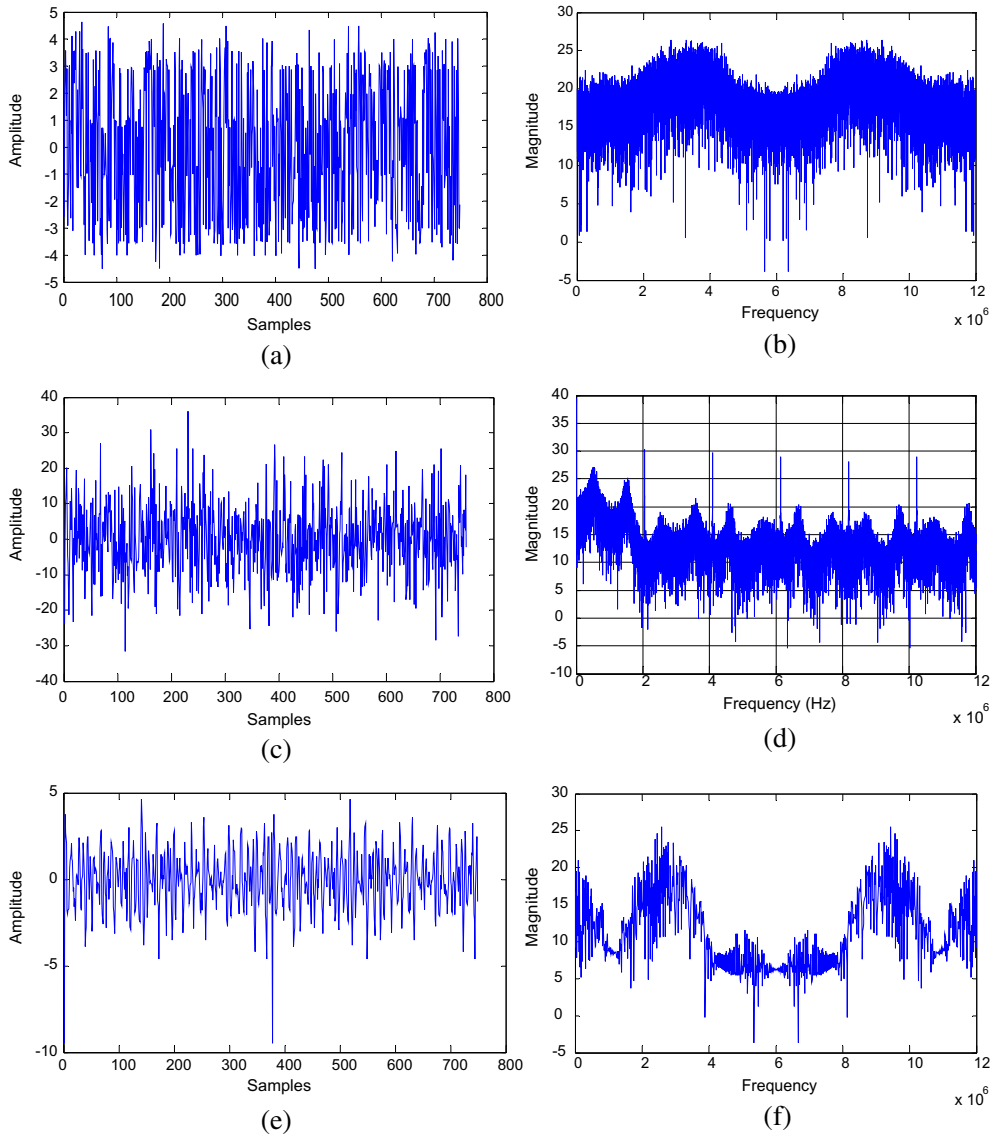


**Figure 2** (a) GPS data of 750 samples, (b) Spectrum of GPS data, (c) impulse noise affected GPS signal with $C/N_0$ 20 dB-Hz, (d) spectrum of noisy GPS data with $C/N_0$ 20 dB-Hz, (e) Impulse noisy signal filtered through spiking filter and (f) recovered spectrum of GPS signal through spiking filter.

generated PRN-3 is correlated with the impulse noise buried GPS signal having a $C/N_0$ ratio of 20 dB-Hz and the probability of false alarm ($pf_a$) is kept at $10^{-2}$. The probability of detection ($P_D$) is computed for different integration periods. Fig. 6 shows the Montecarlo simulation results for 10,000 trials to ensure the effectiveness of the performance comparison between the coherent, non-coherent,

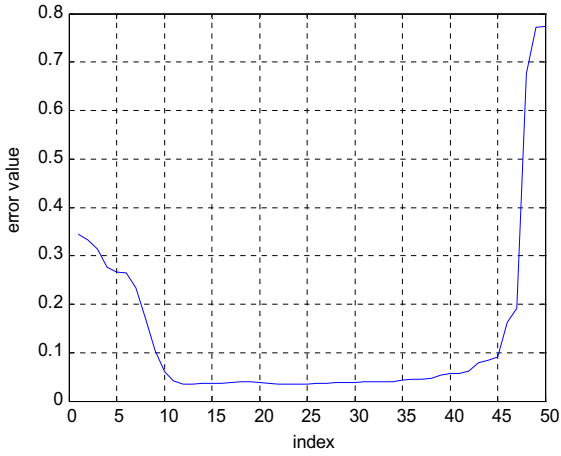


(a) Mean squared error ($J_{min}$) of Performance matrix

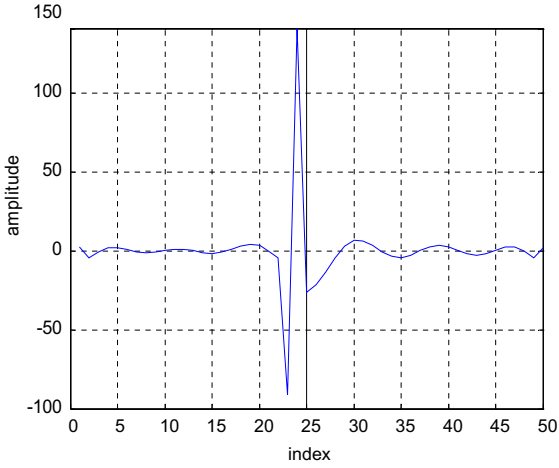


(b) Spiking filter coefficients of order M=50

**Figure 3** Characteristics of spiking filter used.

differential and spiking filter combined differential detection methods. Initially the Coherent detection integration period of 10 ms is analyzed. Due to navigation data transition problem, integration time cannot be extended beyond 20 ms and this method can detect only 35 dB-Hz $C/N_0$ level with 100% of probability of detection. Non coherent integration period of 36 ms gives 100% probability of detection only in the signal range of 30 dB-Hz. Both the methods fail to detect the weak signal at 20 dB-Hz power level. Differential detection also fails to detect the signal and it gives only 50% of detection with the same input power level. The inverse spiking filter integrated with the differential detection performs better and is able to locate the PRN 3 with 90% of detection.

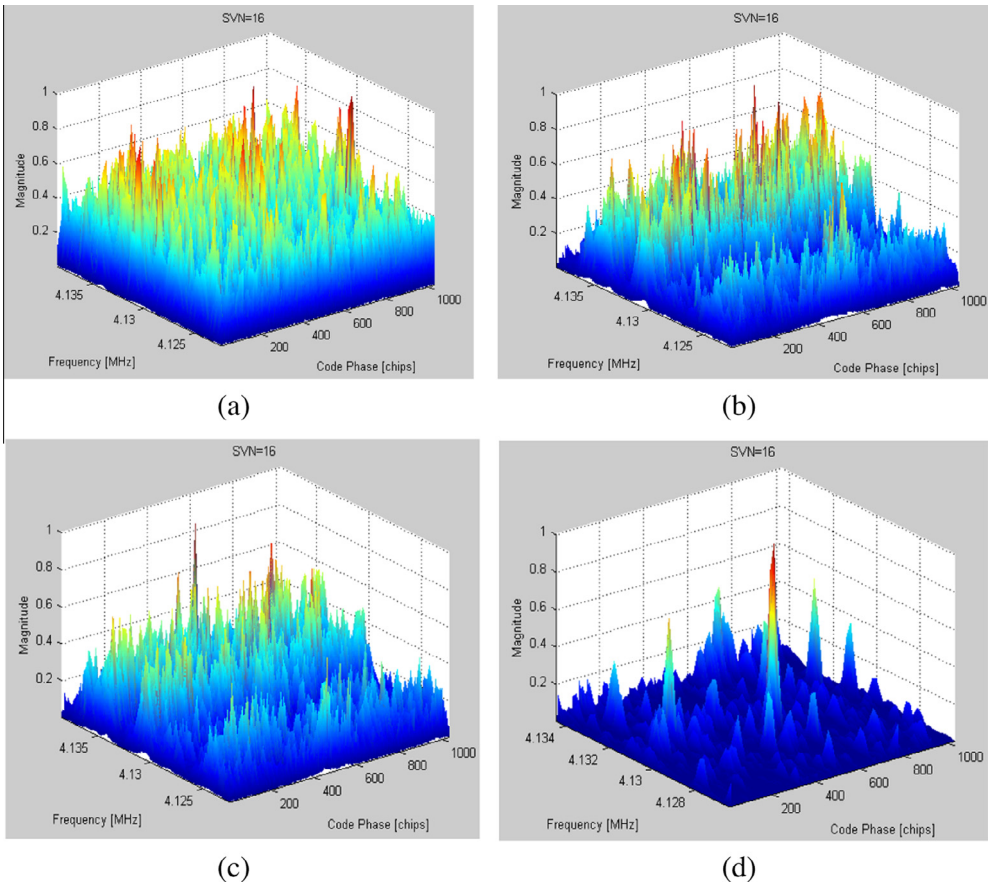


**Figure 4** Correlation output of SVN16 utilizing various conventional methods. (a) Single msec data, (b) coherent detection technique, (c) non-coherent detection technique and (d) differential coherent detection technique.

### *3.3. Software based GPS receiver tracking performance assessment in the presence of impulse noise*

Acquisition stage gives only a rough estimate of the frequency and code phase of a satellite signal. Hence it is required to refine these values in order to confirm whether the acquired satellite metrics is correct or not i.e., code and carrier lock is achieved with the incoming signal to keep track and demodulate the navigation data for a particular satellite. Thus to track a GPS signal, two tracking loops are used. One is code loop known as delay lock loop (DLL) or early-late tracking loop which is used to track the C/A code phase and the another one is phase-locked loop (PLL) which is used to track the carrier frequency of the incoming signal with Doppler shift. Both loops are intercoupled. The impulse noise affected GPS signal is given as the input to the tracking module and in-phase and quadrature part of

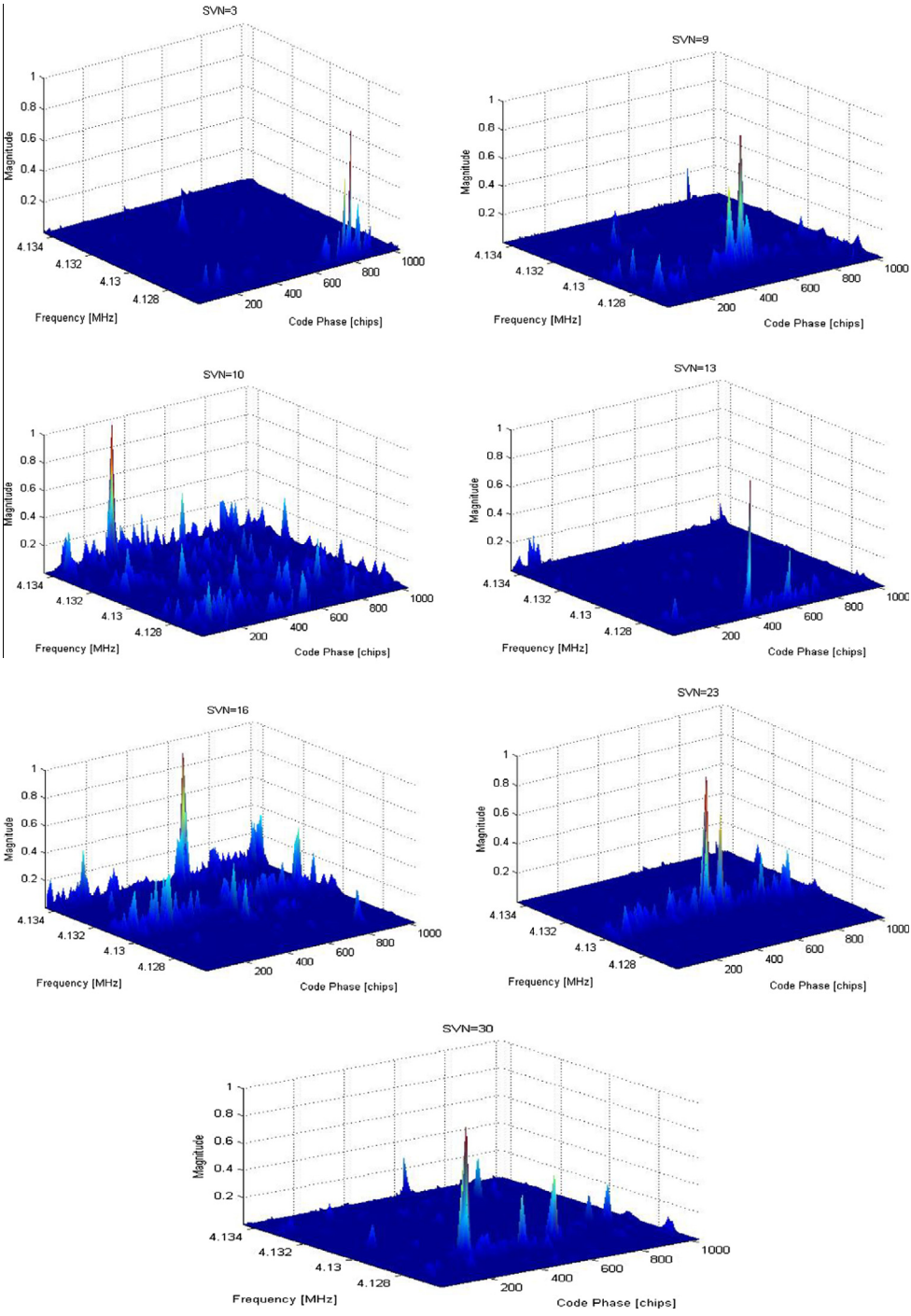


**Figure 5** Correlation outputs of all visible satellites processed by modified differential coherent approach.

**Table 3** Comparison of satellite information for traditional and modified differential coherent method.

| Traditional differential coherent (Fallahi et al., 2012; Mao et al., 2008) | | | | Modified differential coherent | | | |
|---|---|---|---|---|---|---|---|
| SVN | Frequency | Doppler frequency | Code phase chips | SVN | Frequency | Doppler frequency | Code phase chips |
| 13 | 4,126,400 | 4000 | 449 | 3 | 4,126,400 | 4000 | 949 |
| 16 | 4,133,800 | −3400 | 410 | 9 | 4,128,400 | 2000 | 482 |
| | | | | 10 | 4,134,200 | −3800 | 205 |
| | | | | 13 | 4,126,400 | 4000 | 393 |
| | | | | 16 | 4,133,800 | −3400 | 410 |
| | | | | 23 | 4,130,000 | 400 | 523 |
| | | | | 30 | 4,128,400 | 2000 | 227 |

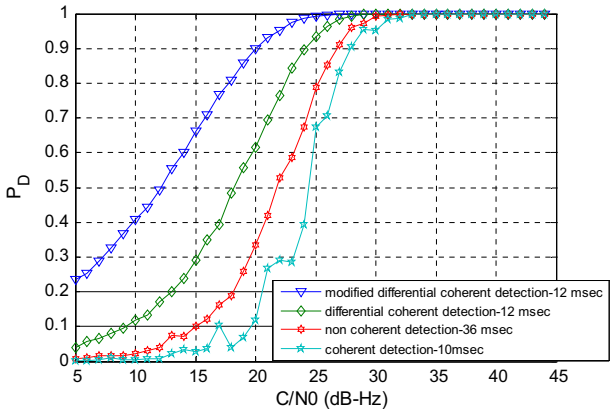


**Figure 6** Performance comparison of various detection techniques.

carrier replica with frequency 3.563 MHz is generated to wipe off the carrier from the input signal. The two equally spaced ($\pm 0.5$ chip apart) early and late versions C/A code of visible satellites [SVN 3, 9, 10, 13, 16, 23 and 30] acquired in the previous section is generated and correlated with the incoming signal to produce two outputs. These outputs are filtered, squared and compared using an early-late normalized envelope discriminator. The phase lock loop (PLL) comprises of a numerically controlled oscillator (NCO), carrier loop filter and a discriminator (Kaplan, 1996). The output of the DLL is a signal only modulated with the navigation data, which is also used as the input to the PLL. The Costas loop is used for GPS signal tracking in the PLL stage. An arc tangent discriminator that is insensitive to the phase transition of the navigation data bit transitions is used to determine the phase shift in the carrier frequency (Kaplan, 1996).The tracking loop parameters used for simulation are listed in Table 4. Once the lock has been accomplished, the navigation data bits are extracted from the In-phase arm since the local carrier signal is in-phase with the incoming signal and all the energy will be in '*Ip*'.

**Table 4** Tracking simulation parameters.

| 2nd Order tracking loops | Code loop | Carrier loop |
|---|---|---|
| Loop bandwidths | DLL:25 Hz | PLL:2 Hz |
| Discriminator type | $\frac{(I_E^2+Q_E^2)-(I_L^2+Q_L^2)}{(I_E^2+Q_E^2)+(I_L^2+Q_L^2)}$ | $\tan^{-1}\left(\frac{Q_p}{I_p}\right)$ |
| Damping factor($\xi$), natural frequency($\omega_n$) | $\xi = 0.707$, $\omega_n = 3.7714$ | $\xi = 0.707$, $\omega_n = 47.1428$ |
| VCO gain ($k_0$), gain of the phase discriminator ($k_d$) | $k_0k_d = 1.0$ | $k_0k_d = 0.25$ |
| Loop coefficients $c_1$, $c_2$ | $c_1 = 5.2901$, $c_2 = 0.0143$ | $c_1 = 25.4974$, $c_2 = 1.9464$ |
| GPS signal power level | 20 dB-Hz | |

The impulse noise affected signal processed through traditional differential detection for SVN-3 is tested for tracking and the performance is given in Fig. 7. SVN-3 is tested during the acquisition phase as this satellite does not satisfy the threshold condition and is an invisible satellite. Here the PLL and DLL errors are not considerably reduced to the minimum extent. The input and reference signals are not in-phase and the *Ip* and *Qp* values contain only noise. The demodulation of navigation data is not possible in this case due to loss of lock with the incoming signal and the tracking fails to demodulate the navigation data. From the results we conclude that the noise is not effectively excised; so reacquisition of GPS data is required.

The tracking operation is next tested for spiking filter combined with differential detection. For this method, the carrier frequency settles after 100 ms period and is shown in Fig. 8a. It is inferred that lock has been achieved for the GPS signal power level of 20 dB-Hz. The code-phase error and PLL error of SVN-3

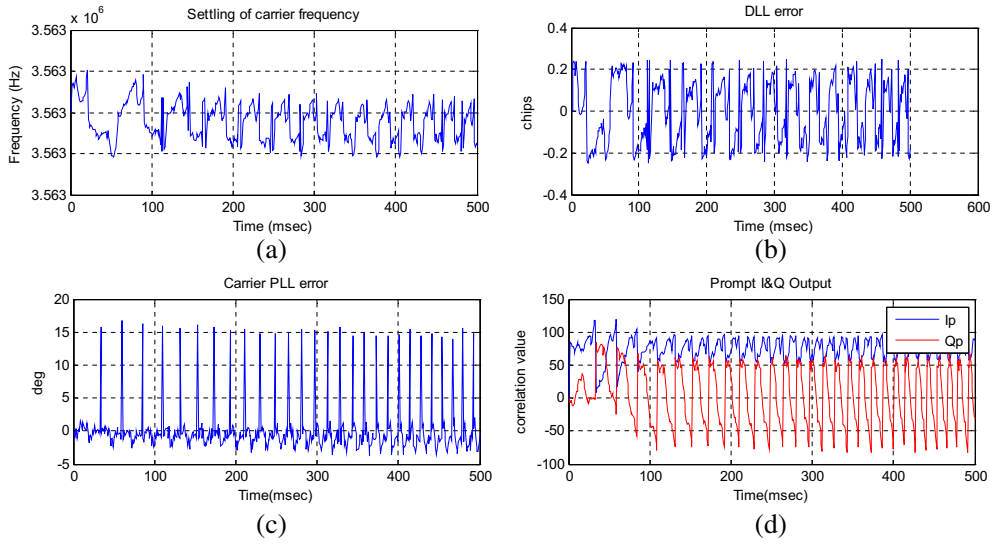


**Figure 7** Tracking loop performance of SVN-3 corrupted by impulse noise processed through differential detection. (a) Settling of carrier frequency, (b) DLL error, (c) PLL error and (d) Prompt *I* and *Q* output.

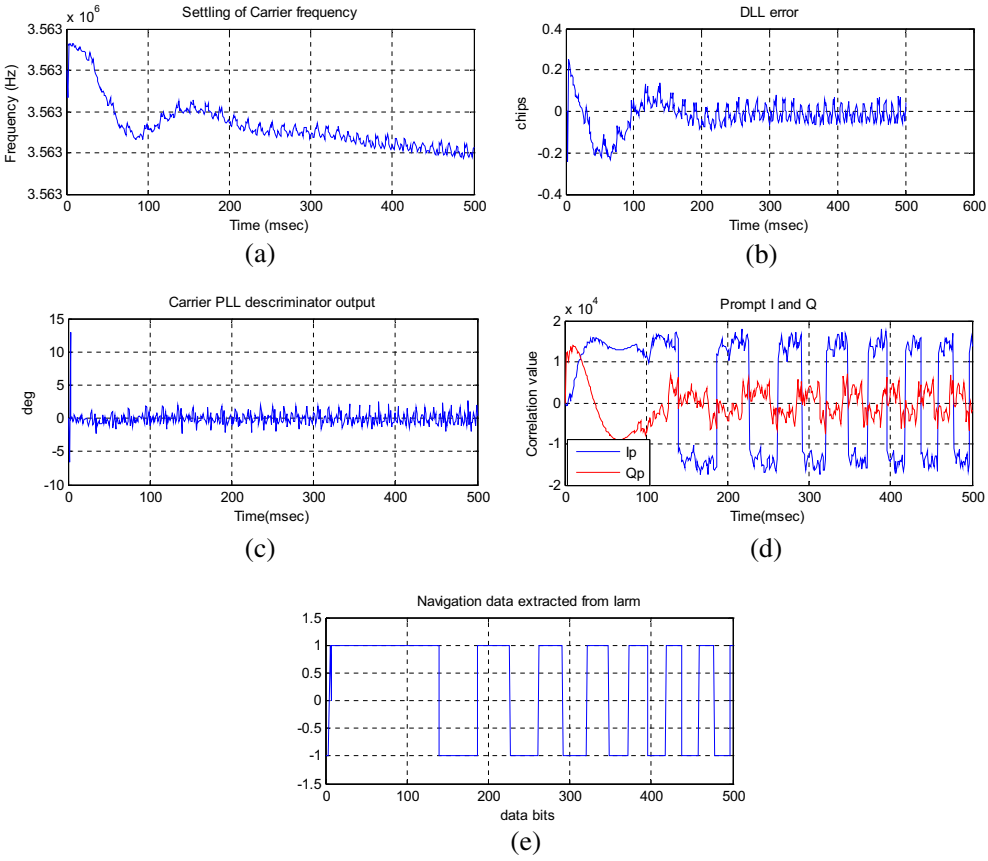


**Figure 8** Tracking loop performance of SVN-3 corrupted by impulse noise processed through spiking filter combined differential detection. (a) Settling of carrier frequency, (b) DLL error, (c) PLL error, (d) Prompt $I$ and $Q$ output and (e) navigation data extracted from $I$ arm.

are plotted in Fig. 8b and c. The outputs show that the code and carrier loops are tracking the incoming signal with good accuracy. When the input and reference signals are in-phase, the $I$ arm only contains the navigation data as indicated in Fig. 8d and the $Q$ arm contains only noise. The binary navigation data demodulated from the $I$ arm are shown in Fig. 8e.

## 4. Conclusion

In this paper, a method based on the least square spiking filter is proposed to excise the impulse noise in GPS receivers. From the results, it is evident that by replacing the traditional differential coherent approach by least square spiking filter, the detection of the number of visible satellites is increased and the reacquisition of GPS data is avoided. It is shown that coherent, non-coherent detections handle the GPS signal with $C/N_0$ only up to 35 and 30 dB-Hz, respectively whereas

differential detection is suitable in the range of 25 dB-Hz. The proposed method efficiently excises the noise and provides 90% of probability of detection for $C/N_0$ of 20 dB-Hz and passes the tracking operation with successful demodulation of the navigation data. Further tracking results can be passed onto the bit and frame synchronization modules to find the user position with good accuracy.

## References

Bao-Yen, James, Tusi, 2005. Fundamentals of Global Positioning System Receivers-A Software Approach, second ed. Wiley-Interscience, Canada.

Borio, Daniele, Camoriano, Laura, Savasta, Simone, Lo Presti, Letizia, 2008. Time-frequency excision for GNSS applications. IEEE Syst. J. 2 (1).

Braasch, M., Van Dierendonck, A., 1999. GPS receiver architectures and measurements. Proc. IEEE 87 (1), 48–64.

Deshpande, S., Cannon, M.E., 2004. Interference Effects on the GPS Acquisition, National Technical Meeting. Institute of Navigation, 26–28, January.

Fallahi, Kia, Wang, Donglin, Fattouche, Michel, 2012. Probability of Outlier Analysis in Weak GPS Signal Acquisition Journal of the Franklin Institute. Elsevier Publications, pp. 1930–1943.

Hu, Hui, Fang, Lian, 2010. Algorithms of signal search and acquisition in software global positioning system receiver. J. Environ. Technol. 3 (1), 30–35.

Kaplan, E.D., 1996. Understanding GPS Principles and Applications. Artech House Publishers, Norwood, MA.

Mao, Wei-Lung, Chen, An-Bang, 2008. New Code Delay Compensation Algorithm for Weak GPS Signal Acquisition International Journal of Electronics and communications. Elsevier Publications, pp. 665–677.

Mathew, R., Narayana Dutt, D., 1993. Wave shaping filters for spectral estimation of short segments of EEG signals. IEEE.

Sophocles J. Orfanidis, 1988. Optimum Signal Processing, An Introduction Second Edition, McGraw-Hill Publishing Company.

Guoliang Zhu, Xiaohui Chen, 2010. An improved acquisition algorithm for GPS signals. J. Commun. Comput. 7 (1), ISSN 1548–7709, USA, (Serial No. 62).